Laboratory measurements of the mechanical behavior of heterogeneous soils

Philippe REIFFSTECK*
Université Paris-Est, Laboratoire central des ponts et chaussées, Paris, France

Jocelyn ARBAUT
Nadège SAGNARD
Matoren KHAY
Centre d'études techniques de l'équipement Normandie-Centre, Grand-Quevilly, France

Didier SUBRIN
Christian CHAPEAU
Laboratoire régional des ponts et chaussées de Lyon, France

Daniel LEVACHER
Université de Caen, France

***CORRESPONDING AUTHOR:**
Philippe REIFFSTECK
philippe.reiffsteck@lcpc.fr

ABSTRACT

One of the main characteristics of coarse-grained soils is the difficulty involved in proceeding with extraction and evaluation of their mechanical properties. This challenge pertains to the size ratio between the diameter of the material's coarsest grain and the smallest test cell dimension. Based on a single given material (in this case, an alluvial gravel), this paper will discuss the results from tests conducted using differently-sized direct shear boxes (reaching up to 500 mm to a side and 600 mm in diameter) and with triaxial devices whose specimen diameter equals 150 or 300 mm, which enables measuring deformations locally. The mechanical behavior deduced from test results will be complemented by other behavioral measurements taken on an instrumented embankment. The objective of this experimental program has been to discern the influence of recomposition compaction modes along with the type of test on the range of mechanical parameters, such as cohesion, angle of internal friction and deformation modulus. A critical analysis of test results will also be presented. Questions related to scale effects will be raised for both types of tests (i.e. shear box and triaxial). As an outcome of this work, it appears that the set of recommendations currently listed in testing standards need to be modified for application to coarse-grained material.

Mesures en laboratoire du comportement mécanique des sols hétérogènes

RÉSUMÉ

La difficulté de prélèvement et d'évaluation de leurs propriétés mécaniques est une des caractéristiques des sols grossiers. Cette difficulté est liée au rapport de taille entre le diamètre des plus gros grains du matériau et la dimension la plus faible de la cellule d'essai. À partir d'un même matériau (une grave alluvionnaire), on présente les résultats d'essais effectués avec des boîtes de cisaillement direct de différentes dimensions (jusqu'à 500 mm de côté et 600 mm de diamètre) et avec des appareils triaxiaux, dont le diamètre des éprouvettes est de 150 ou 300 mm, qui permettent la mesure locale des déformations. Le comportement mécanique déduit des résultats d'essais est complété par d'autres mesures de comportement réalisées sur un remblai instrumenté. L'objectif du programme expérimental était de mettre en évidence l'influence des modes de reconstitution et de compactage ainsi que du type d'essai sur les paramètres mécaniques comme la cohésion, l'angle de frottement interne et le module de déformation. Une analyse critique des résultats des essais est présentée. Les questions d'effets d'échelle sont abordées dans les deux types d'essai (à la boîte et au triaxial). Il apparaît que les recommandations inscrites actuellement dans les normes d'essais devraient être modifiées afin de pouvoir les appliquer aux matériaux grossiers.

INTRODUCTION

Coarse-grained material, by virtue of containing larger-sized granular elements, are very difficult to sample in a way that leaves the grains intact or to characterize from a mechanical perspective using the conventional equipment and instruments found in a laboratory. Consequently, designing the

geotechnical structures that incorporate such materials (i.e. foundations, retaining walls, embankments, dams) raises a number of unresolved concerns. In light of this context, a research program was undertaken on coarse-grained soils within the LPC network of civil engineering laboratories, in the aim of determining the respective influences of the mode of recomposition, the mode of compaction and the type of test on typical mechanical parameters. As an example, the importance of deriving values for cohesion and the angle of internal friction of coarse-grained soils becomes evident when calculating the stability of hillside slopes or structures. The research performed as part of this program makes use of a wide range of studies completed within the LPC network **[1-3]**.

The bibliographical analysis included herein indicates that the parameters exerting an influence on the behavior of coarse-grained soils are: mass density, particle type and shape, particle size distribution, range of particle sizes, content and quality of the fines coating the larger granular elements, water content, and test equipment dimensions **[4]**.

Many authors have examined the influence of relations between the size of the test instrument (L_0 for the shear box, D_0 for the triaxial device) and the size of the largest particle (d_{max}) on the behavior of a coarse-grained soil. They have verified that this relation did play a sizable role in the shear strength of a coarse-grained material. Direct shear tests have thus been conducted in varying:

– box size: Fry *et al.* **[5]** used both a square box of side length 1,200 mm and a round box 100 mm in diameter in order to run tests on a highly brittle sandstone with a siliceous matrix displaying a maximum diameter of 160 mm;
– particle size distribution curve: Santos *et al.* **[6]** prepared, from the same material sample (d_{max} = 25 mm), three materials with parallel particle size distribution curves to carry out direct shear tests using the square shear box of side length 300 mm.

These tests serve to highlight the strong influence of equipment size on experimental results. The influence on angle of friction is expressed as a function of the scale factor L_0/d_{max} **(see Fig. 1a)**. The values of L_0/d_{max} vary between 8 and 240. The angle of friction decreases as L_0/d_{max} rises and then stabilizes for L_0/d_{max} values greater than 50. A considerable increase in the angle of friction is obtained for L_0/d_{max} values below 25. These results have been confirmed by tests performed by Vallé **[4]** on a coarse-grained alluvial material from the town of Crest (Drôme, southeastern France).

A similar study was undertaken using the triaxial device **(Fig. 1b)**, i.e.:

– Fumagalli **[7]** ran triaxial tests with a specimen diameter D_0 equal to 100 mm on a limestone with various particle gradings;
– Holtz and Gibbs **[8]** carried out triaxial tests on specimens with diameters of 35 mm, 82.5 mm, 152 mm and 229 mm composed of mixes of gneiss, granite and schist gravel with a diameter d_{max} of 19 mm, as well as on a sand with a d_{max} diameter dimension of 4.76 mm.

figure 1
Angle of friction vs. scale factor (D_0/d_{max} and L_0/d_{max}):
- a: direct shear tests
- b: triaxial tests

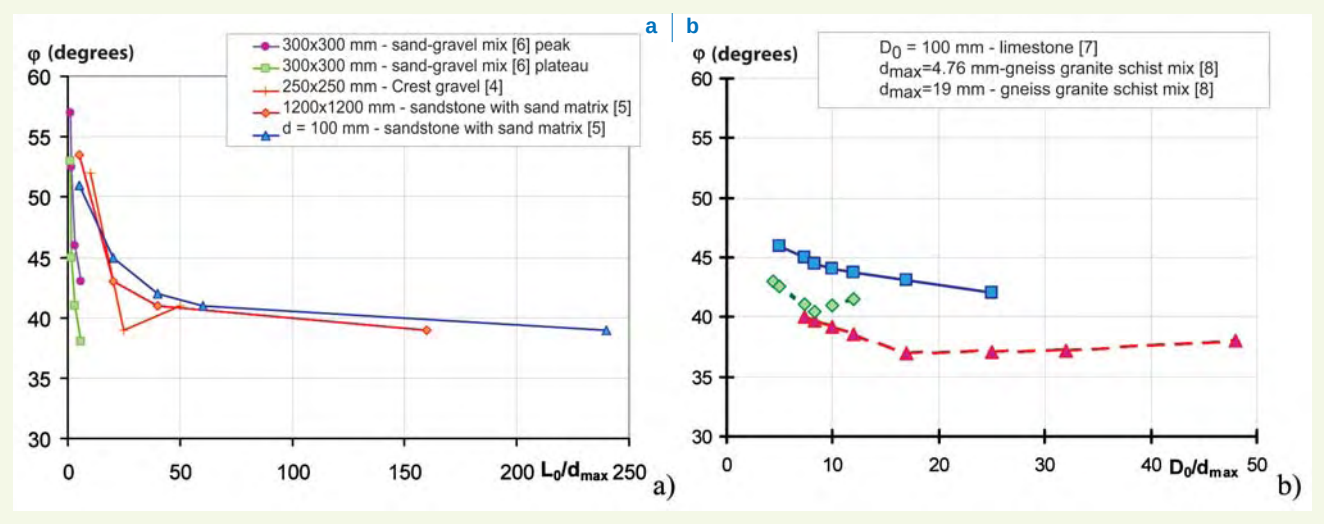

They obtained a drop in the angle of internal friction when increasing the D_0/d_{max} ratio. This reduction is particularly strong for $D_0/d_{max} < 10$ values.

It can thus be concluded from these studies that the scale factor L_0/d_{max} must lie above 15 or 20 for the shear box test when the material displays a flattened particle size distribution curve and twice this value when particle graduation is uniform. For the triaxial device, the D_0/d_{max} ratio must equal 6. A higher ratio could be acceptable when the material offers a uniform particle size distribution.

The void index, which is correlated with the dry mass density, serves as another key parameter. The angle of internal friction is thus higher for soils composed of angular particles than for those formed with more rounded particles, with the average deviation amounting to 10 degrees **(Fig. 2a)**. Moreover, the angle of friction increases with a rise in the uniformity coefficient (C_U). The geological origin of the material also exerts an influence on mechanical behavior; angle of friction values are greater for limestone-based materials than for siliceous limestone materials **(Fig. 2b)**.

This research mission was intended to evaluate the pertinence of rheological models adapted to such materials and of the procedures employed to determine their parameters either in the laboratory or *in situ*, in the ultimate aim of comprehending the material behavior within actual structures, i.e.: stability, deformation. Once a natural reference material was chosen, a parametric testing campaign was held so as to introduce various widely-used recomposition techniques, along with several instruments suitable for testing coarse-grained soils and an experimental embankment designed to serve as a reference. Special attention was paid to the influence of both the recomposition and compaction modes and to the type of test on mechanical parameters, such as cohesion, angle of internal friction and deformation modulus.

It can be noted that a natural granular assembly, as qualified by the *in situ* grain distribution and configuration, depends on how the deposit originated and, under no circumstances, can be accurately reproduced in the laboratory.

figure 2
Influence from the shape (a) and nature (b) of grains on the angle of friction

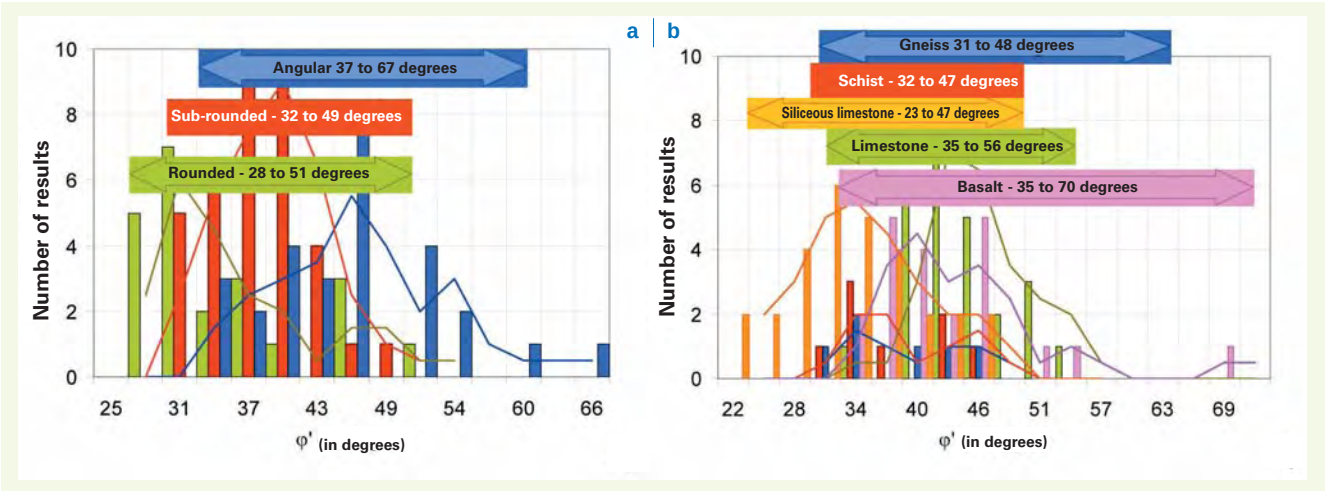

PRESENTATION OF THE EXPERIMENTAL WORK

Material description and characteristics

The reference material selected for this study is a crusher run of natural 0/80 mm gravel drawn at an alluvial sand-limestone deposit from the Seine River Valley terrace, and more specifically from the Criquebeuf-sur-Seine Quarry (Seine-Maritime, Normandy) **(see Table 1 below)**.

table 1
Characteristics of the material drawn from Criquebeuf-sur-Seine

Material	Natural	Leveled at 50 mm	Leveled at 25 mm	Removal / Substitution at 25 mm
d_{max} (mm)	80	50	25	25
% < 80 µm	8.3	11.2	10.4	8.7
% < 5 mm	54.2	68	67.8	55.5
C_U	91	70	32	70
C_C	0.12	0.52	0.58	0.30

The particle size distribution curves of the 0/80 mm gravel and both the 50- and 25-mm leveled fractions are shown in **Figure 3**. It can be observed that the study material displays a "mount", which is a common characteristic among siliceous limestone gravel from the Seine River Valley; this lump becomes more accentuated with the presence of limestone, as well as with the abundance and distribution of flint. This unique trait is reflected by the low values found for the curvature coefficient $C_C = d_{30}^2/d_{10}.d_{60}$. The average particle size distribution curves of the materials have also been presented after removal of the 25/80 category and substitution by the same weighted quantity of 6.3/25; furthermore, particle size distribution curves are shown for the materials used in constructing the experimental embankments, screened with a quarried materiel for leveling at 25 mm. The first embankment (called the "small embankment"), which will be described in this article, is of more limited dimension and was preliminarily built in order to validate the feasibility of the actual test embankment (simply called "embankment").

figure 3
Average particle size distribution curves for the study materials

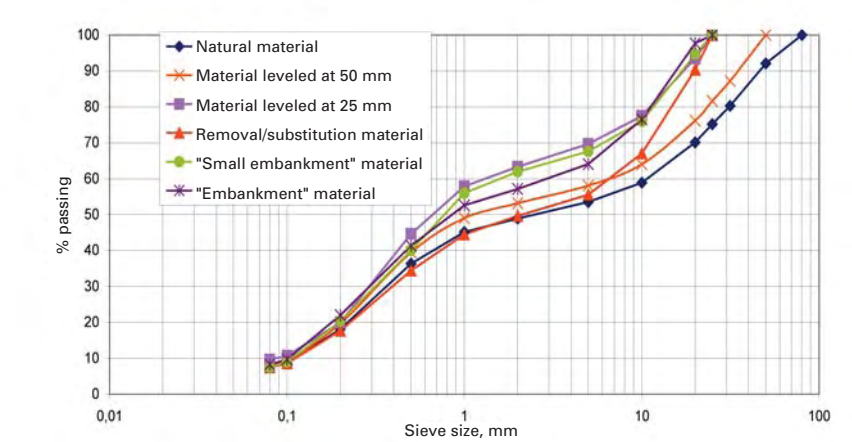

Shear box tests

› 500-mm square shear box

Within the scope of this research program, the majority of tests have been conducted in a square cross-section direct shear box at the Rouen Road Testing Center (CER). This prototype set-up was developed by the Rouen Prototype Testing and Design Center (CECP) during the 1990's, with a side length of 500 mm that could be reduced to 250 mm **(Fig. 4)**, composed of half-boxes 150 mm and 100 mm high, respectively, separated by a spacing (t) **[4]**. In order to obtain the 250-mm box, two 250-mm half-boxes are placed into the 500-mm box fitted on the equipment, with a total height of 200 mm (100 mm for each half-box). At the bottom, a plate 40 mm high is positioned to ensure that the specimen has the same thickness in the lower part as in the upper part. The shear box tests are carried out on unsaturated material specimens, set into place with both a water content and mass density that had been previously set by the experimenter.

a | b

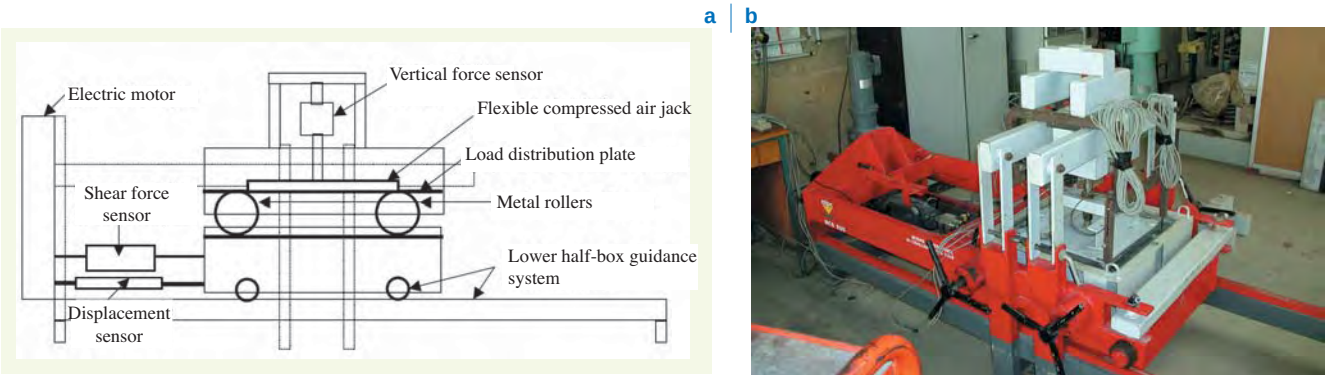

figure 4
Direct shear box with a square cross-section produced by the Rouen-based CER Test Center:
- a: operating principle
- b: overview

The shear test machine is supported by a metal frame. A flexible pneumatic jack serves to exert the vertical compressive force. The chassis element provides for the box guidance system. The lower half-box moves during the test and a jackscrew, driven by an electric motor whose controls include the setting and adjustment of shear speeds, provides the tension.

The specimens were produced in three successive layers with thicknesses of:

– 90 mm, (100 + t) mm, and 60 mm for the 500-mm box;
– 35 mm, (60 + t) mm, and 30 mm for the 250-mm box.

The second layer is always centered at the level of the shear surface. Specimen height always equals half the box dimension plus the spacing between the two half-boxes.

The spacing (t) introduced between the two half-boxes is a critical parameter in the direct shear test on soils with a high diameter d_{max}. As indicated by Laréal *et al.* **[9]** and Bourdeau *et al.* **[10]** and then discussed by Shirdam *et al.* **[11]** and Vallé **[4]**, this spacing when set too small would seem to limit the separation of particles in the shear plane and lead to high apparent cohesion. The spacing (t) was set at $d_{max}/2$ for all of the tests described below. Spacing values of 25 mm, 12 mm, 6 mm and 5 mm were used for materials featuring respective diameters d_{max} of 50 mm, 25 mm, 12.5 mm and 6.3 mm.

› Round shear box 600 mm in diameter

The shear test machine for coarse-grained soils used at the Lyon regional *Ponts et Chaussées* laboratory (LRPC) has also been placed into service to perform a portion of the tests on Criquebeuf alluvial gravel. This machine, also a prototype, was built by the Angers Prototype CECP Center during the 1970's on the basis of a set of specifications developed by LRPC. Such a device is commonly used to test component materials of reinforced soils. The testing principle is inspired from that of the Casagrande direct shear box, yet with dimensions better adapted for testing materials featuring coarse elements without inducing scale effects capable of altering results interpretation. This paper will concentrate on the test equipment, the operating principle, specimen introduction and the testing protocol **[12]**.

Shear machines are conventionally equipped with a vertical loading system that acts through a stiff plate. The LRPC machine design relied on applying a vertical force via a pneumatic jack, with the advantage of a flexible transmission of forces at the top of the specimen. The schematic diagram is depicted in **Figure 5a**.

The actual box is composed of two steel half-boxes 600 mm in diameter and 300 mm high. The test machine **(Fig. 5b)** features a mechanically-welded metal frame comprising both the housing and the mobile plate that accommodates the lower half-box. The spacing between half-boxes is set during the test procedure by raising the upper half-box which is held stationary thanks to a gooseneck.

The vertical loading (maximum stress of 600 kPa) is implemented by means of a pneumatic jack that applies stresses to the test material via a rubber membrane and a Plexiglas disc. The horizontal

a | b

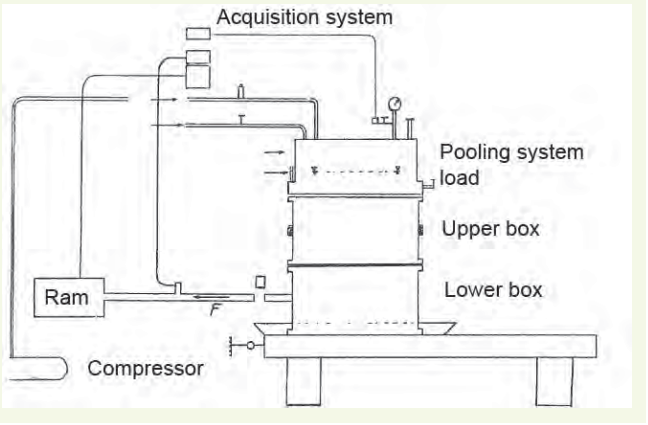

figure 5
Direct shear box with a circular cross-section produced by the Lyon regional Ponts et Chaussées laboratory:
- a: operating principle
- b: overview

loading system, which exerts a tensile force (max. 200 kN) on the lower half-box, contains a mechanical jackscrew actuated by an electric motor with shear speeds held constant throughout the test. The speeds *v* are ascribed one of the following values: 0.5, 1, 1.5, 2, 3 or 5 mm/min.

The measurement system adopted for the two types of boxes is composed of:

– a force sensor, with digital display, for measuring the tangential force;
– a manometer (pressure sensor) for measuring the normal stress;
– a comparator for measuring the relative tangential displacement between half-boxes; and
– sensors for measuring sample settlement during the consolidation period.

Triaxial tests

› Triaxial device with a diameter of 150 mm

Created as a reference test to determine soil shear strength, the triaxial test was performed herein for the first series of tests with a conventional triaxial set-up. The triaxial revolution device is composed of a triaxial cell and a loading system containing a press and various pressurization and measurement instruments **(see Fig. 6)**. A set of consolidated triaxial tests were performed on the unsaturated 150-mm diameter specimens, in accordance with Standard NF P 94-074 **[13]**. The isotropic consolidation step lasted 15 hours and proceeded with application of a stress corresponding to the selected radial stress (50, 100 or 150 kPa). The shear testing speed was set at 0.1 mm/min, until reaching a 10% deformation threshold.

The use of instrumentation that enables locally measuring both axial and radial deformations serves in this set-up to derive the deformation modulus from measurements taken over the central part

figure 6
Triaxial test equipment and specimen instrumentation at the Rouen regional Ponts et Chaussées laboratory:
- a: overview
- b: detailed drawing of the measurement cell

a | b

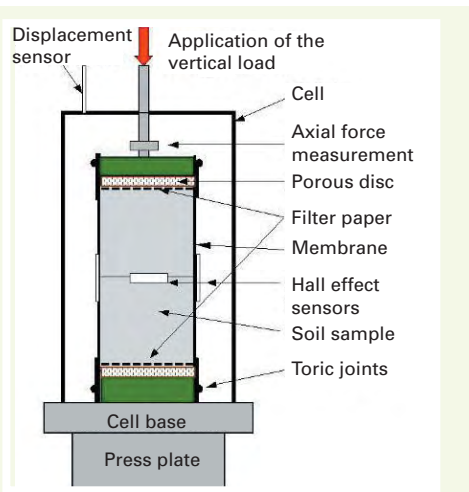

figure 7
Specimens fitted with a local system for measuring axial and sheared deformations

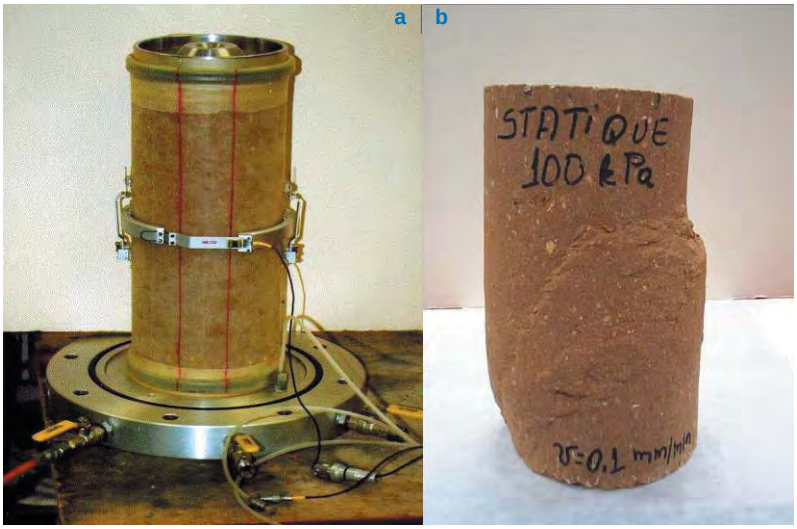

of the specimen, i.e. the zone where deformations are the most homogeneous, and to assess the variation in volume even for unsaturated specimens or to maintain the diameter constant when running a Ko-type test **(Figs. 7a** and **b)**.

› Large-sized triaxial device

A second series of tests was conducted using a large-sized triaxial set-up. In 1968, the Rouen-based prototype workshop first developed a triaxial device featuring large dimensions to enable performing tests on reconstituted soil specimens 300 mm in diameter and 600 mm high **(Fig. 8)** **[14]**. This apparatus was reactivated in 2000 by the CECP Center in Rouen **[15-17]**, in the aim of offering the capability of running tests at a constant deformation speed or with an imposed stress or strain path. Given its associated specimen geometry and technical capacity under static loading, this device is comparable to that developed by the CERMES Soil Mechanics Research Center **[18]**.

The structural specificity of this instrumentation set-up is that the cell is not incorporated into a reaction housing, like it is for the conventional apparatus described above; it has been laid out with peripheral tie rods that generate the required reaction. A special cabinet is included to combine the motor assembly, electronic system and hydraulic circuit.

The axial displacement function at constant speed (ΔH) is generated by a motor and a electromechanical clutch-actuated gearbox. It enables obtaining a displacement speed range split into five intervals, between 0.1 micron/min and 10 mm/min.

This press configuration is completed by two "pressure volume controllers" (PVC), each with a 5-liter capacity, in order to keep both the cell and sample pressurized **(see Fig. 8b)**. One PVC ensures a cell loading within the range of 50 to 1,200 kPa, while another, which is identical to the one serving to maintain the pressure σ_c in the cell, provides for pore water pressurization inside the specimen.

Pore pressure is measured by a sensor positioned as close as possible to the specimen base. The vertical force is measured by a sensor embedded in the cell in order to avoid friction on the piston. Three specimen deformation measurement systems have also been implemented, namely:

– global measurement of the variation in specimen height ΔH: this value is measured outside the cell on the mobile piston. Its maximum amplitude is 15%, i.e. 90 mm;
– local measurement over the middle third of the specimen: due to the large dimensions of the specimen, these local measurements will enable reaching the domain of small deformations **(Fig. 9)**.

This measurement system focuses on variations in the central boundary (with the sensor inserted into a crown that surrounds the specimen) and two heights (on two opposite generatrices); and
– measurement of the volume variation ΔV based on the absorbed or expulsed pore water volume (on the backpressure circuit) with PVC piston displacement.

figure 8
Large-sized triaxial testing device:
- a: overview with control box
- b: PVC

a | b

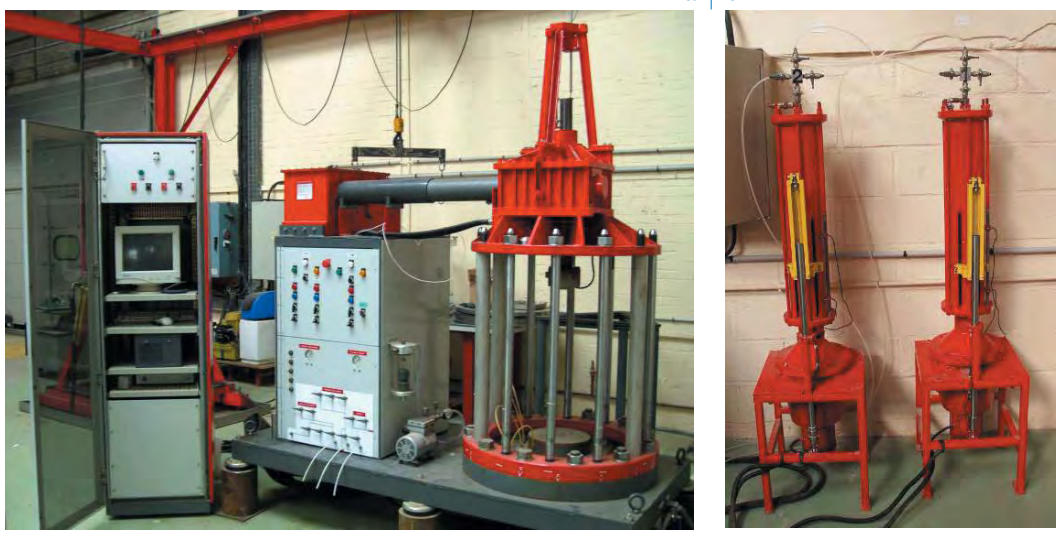

figure 9
Installation of local measurement system on the middle third of the specimen

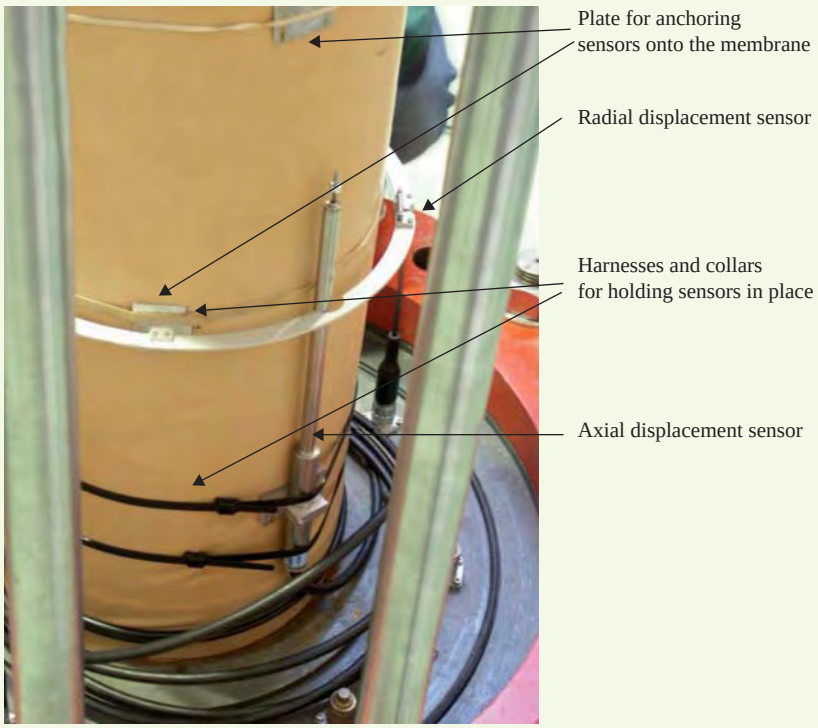

MATERIAL RECOMPOSITION PROTOCOLS BY MEANS OF COMPACTION

The various compaction protocols both in the laboratory and *in situ* have been defined so as to replicate actual worksite conditions as closely as possible **[15]**. These protocols have been used to recompose specimens for the triaxial tests on 150-mm specimens. A key to this study has consisted of building an experimental embankment that reproduces worksite implementation conditions whereby specimens have been extracted block by block. In conjunction with this protocol, the embankment has undergone tests usually conducted to determine effective material implementation.

Quasi-static compaction

For the quasi-static compaction, a laboratory specimen molding press was used. The specimen was compacted into a single layer by means of a piston applying a 40-kN vertical load within a metal mold **(Fig. 10a)**. A certain quantity of material, with a known water content and mass, was then introduced into the mold containing a specified volume and fitted with a metal base (i.e. the Proctor test spacing disc). The compaction procedure consists of having the piston penetrate into the mold, which is supported on the metal base. The mold is then turned upside down and the piston is applied on the other side. This procedure was repeated until the point of maximum possible deformation and allowed obtaining 97% to 98% of the maximum mass density from the normal Proctor test.

Compaction by vibrocompression

A vibratory compression system was introduced to produce laboratory specimens of a predetermined density and water content **(Fig. 10b)**. Both the mold and the material it contains are submitted to the effects of a simple compression directed along the cylinder axis and of a forced vibration whose multidirectional resultant is contained within a plane perpendicular to this same axis. The combined action of this compression and vibration causes a rearrangement of the soil, which then leads very quickly to the desired compactness levels. Compaction occurs within a single layer.

Compaction by vibrating hammer

The material was compacted into three layers using a vibrating hammer equipped with a compaction rammer composed of a cylindrical ramming block 150 mm in diameter. A latex membrane (identical to that used in the triaxial test) is then set inside the mold in order to minimize soil-mold friction. A thin layer of grease is placed in between the mold and membrane so as to reduce the coefficient of friction. The load is applied over the entire specimen surface and the operation is monitored by means of a height control system for each layer. The compaction membrane was removed for purposes of running the triaxial test.

Compaction with the Proctor hammer

For this protocol, the same mold and specimen preparation method were used as for the compaction by vibrating hammer. The material was compacted into three layers herein with the so-called "modified Proctor hammer" by striking each layer 56 times **(Fig. 10c)**. The compaction energy corresponds with that of the normal Proctor test. Following compaction, the surplus material was trimmed back to the level of the mold and the membrane was removed to conduct the triaxial test.

figure 10
Recomposed specimens by means of: a) static compaction; b) vibratory compression; c) the Proctor hammer; and d) cut from the embankment

a | b

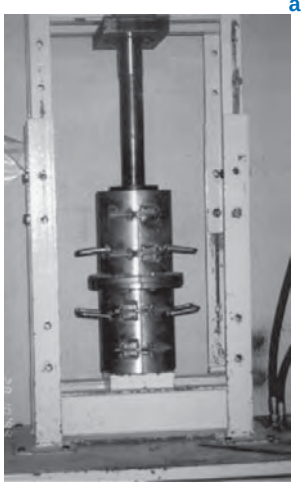

c | d

Embankment compaction

An 18-m^2 embankment was built in three compacted 35-cm layers. The material was set into place with a natural water content (i.e. w = 9.3%) very close to the optimal content determined from the normal Proctor test (w_{NPO} = 9.2%). The compaction protocol defined in the Road Earthworks Guide was applied in order to achieve densification objective q_4, i.e. 95% of the Normal Proctor Optimum (NPO) **[19]**. For each 45-cm layer of material spread, a VP-12 roller was run four times over **[19]**.

This embankment underwent many tests. Its geometry was monitored by means of optical leveling on each layer at 10 different points. Density was controlled using a single-beam, variable-depth gamma densitometer (GPV 25-40) at four points for the lower layer and by a GDS 200 dual probe at two points for the entire embankment thickness. Mechanical testing comprised three tests with the PDG 1000 dynamic penetrometer, three tests run with the 600-mm diameter plate and two pressuremeter tests **(Fig. 11)**.

A total of twelve specimens were cut by hand onsite for the triaxial tests using a 152-mm diameter guide tube; these specimens served as references to assess the protocols applied in the laboratory **(Fig. 10d)**.

figure 11
Measurements performed on the embankment:
- a: using the dual probe,
- b: with the dynamic penetrometer,
- c: by running the plate test

Specimen compaction for tests run using the large-sized triaxial device

Due to its large dimensions, the 300-mm triaxial device has caused a number of specific specimen recomposition problems. From the time of its service startup, a special compaction housing has had to be built and used for tests conducted on reconstituted soils. The specimen recomposition method had necessitated examining the number of layers to be implemented: 3, 6, 10 and 15. Compactness measurements derived from the gamma bench had been recorded on some specimens **[20]**.

The specimen production protocol using the former, renovated compaction housing **(Fig. 12)** was revised after the production tests performed between 2003 and 2005 **[21-22]**. The material is compacted into three 20-cm layers in a mold composed of two half-shells; compaction is carried out with the piston hammer with a mass of 200 kg affixed onto a 50-Hz unbalanced vibrator.

A full disc is fastened at the bottom of the mold in order to retain the material, and a rigid cutout geomembrane is slid inside in order to avoid friction between mold and soil. A 10-cm elevation rise is necessary to apply the last expanded layer **(Fig. 13)**.

Outside of the compaction housing, each material layer is poured into the mold all at once to obtain maximum layer homogeneity. To proceed, a conic pluviation system with a hatch is used with a drop height chosen to be identical for all three layers (680 mm) and then adjusted using a forklift. This

procedure, by approximating as closely as possible a pluviation system for the laboratory triaxial test, enables minimizing the influence of various parameters (operator, material spreading, flow rate, etc.).

Once the material has been poured, the mold is affixed onto the compaction housing and then vibrated for 90 seconds. Following compaction, the mold is transported into the triaxial cell; the two half-shells are opened and the rigid geomembrane is removed. Next, the upper drainage disc is installed and the latex membrane is plated against the specimen using a pressure clamp **(Fig. 14)**. The various phases of the triaxial test take place once the cylindrical enclosure has been installed.

a | b

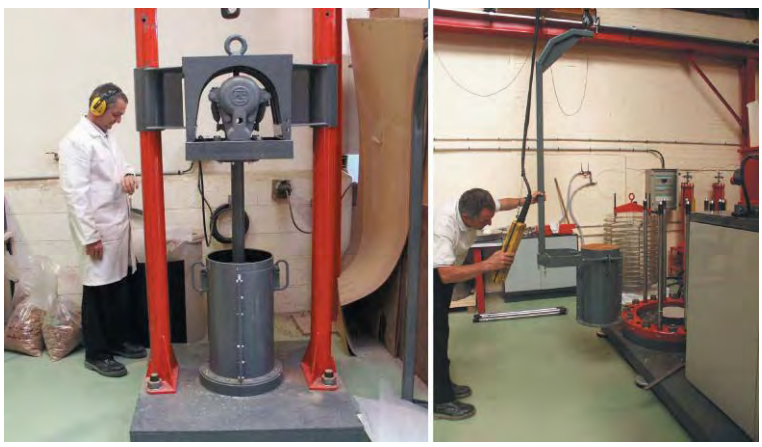

figure 12
Specimen production: a) with the compaction housing; and b) installation within the large-sized triaxial testing device

a | b

figure 13
Mold:
- a: elevation rise
- b: geomembrane

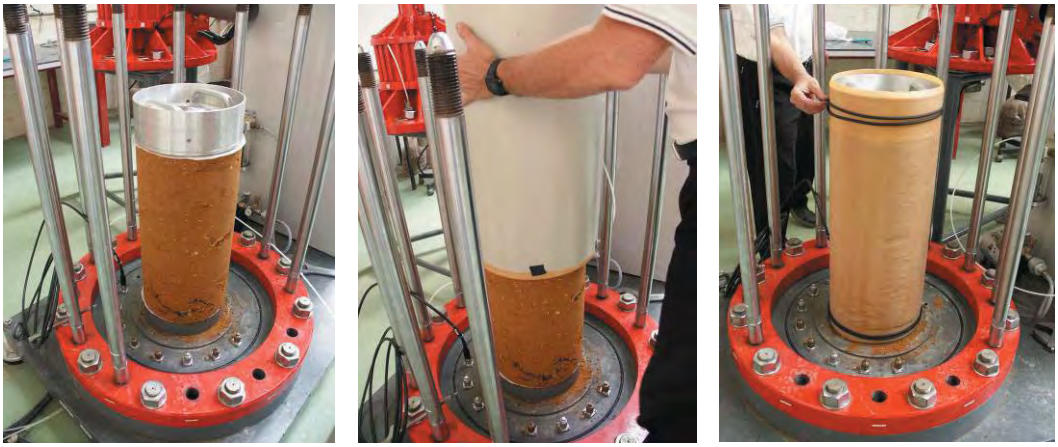

figure 14
Successive phases of specimen placement into the large-sized triaxial cell

INFLUENCE OF STUDY PARAMETERS ON THE MECHANICAL CHARACTERISTICS

The test program has been laid out to study the influence of recomposition mode (leveling vs. removal of the coarse fraction and substitution by a finer fraction), compaction mode (static, vibrant, Proctor,

etc.) and test type (shear box vs. triaxial device) on mechanical parameters such as cohesion, angle of internal friction and deformation modulus.

Influence of recomposition mode on mechanical parameters

The influence of the material recomposition technique on results obtained with the shear box has been investigated **(Fig. 15)**. The materials introduced are of the following granular categories: 0/50, 0/25, 0/12.5 and 0/6.3, either with or without removal and substitution, as indicated in **Table 2**; they are compacted in three layers using a vibrating hammer. Even though tests are conducted systematically, a certain amount of dispersion is still noticed in the results.

An increase in soil shear strength is observed with the jump in grain size at the leveling threshold. This rise is recorded on two parameters: cohesion and angle of internal friction. The angle of internal friction however only varies slightly whereas cohesion increases as parameter d_{max} reaches greater values **(Table 2)**. This behavior may be ascribed to the meshing of grains, which cause the soil mass density to vary. To a certain extent, soil mass density rises with the material grain diameter.

The materials obtained by leveling and removal / substitution at $d_{max} = 50$ mm yield identical values of cohesion *c* and angle of friction φ at the same mass density and water content. This conclusion still needs to be weighted by the test result for $d_{max} = 25$ mm. As a result, a conclusion can only be drawn for one variation direction of angle of friction with d_{max}, while it seems that coarse particle interlocking generates an apparent cohesion. The greatest evolution in cohesion with d_{max} is observed for the removal and substitution technique at $d_{max} = 25$ mm.

The results from **Table 2** have been presented graphically in **Figure 16**, which depicts the cohesion and angle of friction vs. d_{max}. The test result with $d_{max} = 25$ mm for the removal-substitution mode

figure 15
Intrinsic curve for the direct shear box test

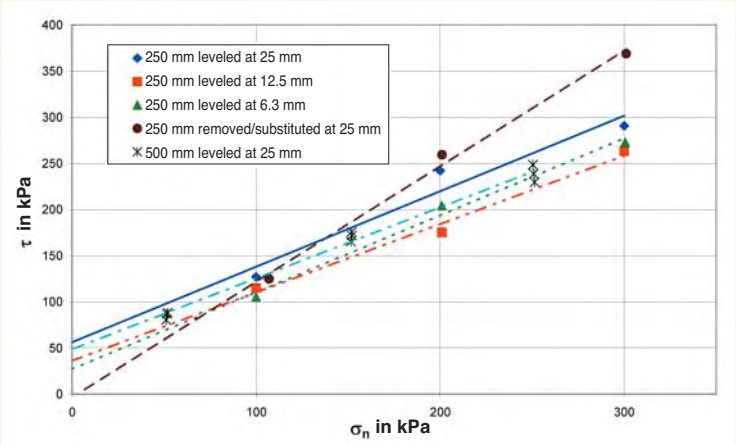

table 2
Results from the shear box tests **[4]**

Mode	Box size	c (kPa)	φ (degrees)	w (%)	ρ_d (t/m³)
Leveling at 25 mm	250 mm	56.5	39.2	8.4	1.99
Leveling at 12.5 mm	250 mm	36.0	36.6	9.4	1.94
Leveling at 6.3 mm	250 mm	26.8	39.8	9.7	1.93
Removal/Substitution at 25 mm	250 mm	7.5	50.6	7.9	1.99
Leveling at 50 mm	500 mm	65.3	45.6	6.3	2.09
Leveling at 25 mm	500 mm	56.1	38.8	7.7	2.03
Removal/Substitution at 50 mm	500 mm	59.7	43.2	6.3	2.07

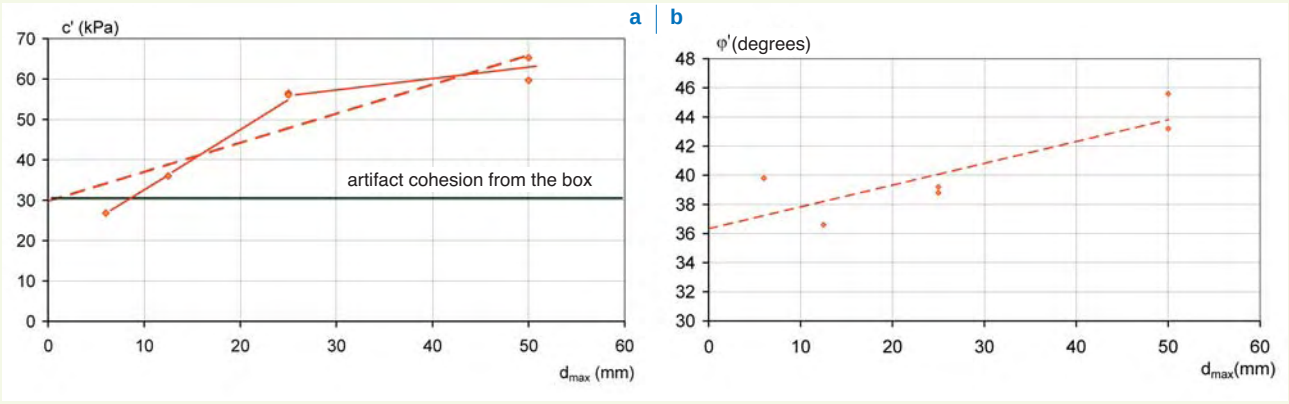

figure 16
Influence of the maximum grain diameter on the c'(a) and φ'(b) shear strength parameters

has been deliberately neglected since it obviously reflects a very distinct and noteworthy criterion, especially by the result with a vertical stress of 300 kPa, as shown in **Figure 15**.

The extrapolation of this result towards a hypothetical material such that $d_{max} = 0$ leads to an angle of intergranular friction on the order of $\varphi_{\mu} = 36$ degrees. This angle has been considered by some researchers as a component of the material's angle of internal friction φ' as a function of density **[23,24]**. For an "ideal" material of this type such that $d_{max} = 0$, the cohesion *c* is zero; this interpretation underscores the presence of an artifact cohesion from the experimental device on the order of $c_0 = 30$ kPa, which agrees with Shirdam's observations **[12]**. These results allow expressing the material shear strength in the following form:

$$\tau_f = c\,(d_{max}) - c_0 + \sigma_n \tan(\varphi\,(d_{max})) \qquad (1)$$

where:

$$\tan\varphi\,(d_{max}) = \tan\varphi_{\mu} + \lambda_{\phi}\, d_{max}$$

$$c\,(d_{max}) = c_0 + \lambda_c\, d_{max}$$

The shear strength normalized by the vertical stress state can then be written as follows:

$$\tau_f/\sigma_n = \tan\varphi + (c - c_0)/\sigma_n \qquad (2)$$

with $c_0 = 30$ kPa being the box artifact.

Figure 17, which displays the evolution in normalized shear strength (for a vertical stress of 100 kPa), reveals that the variation in both angle of friction and cohesion may be integrated with

figure 17
Normalized shear strength vs. dry mass density

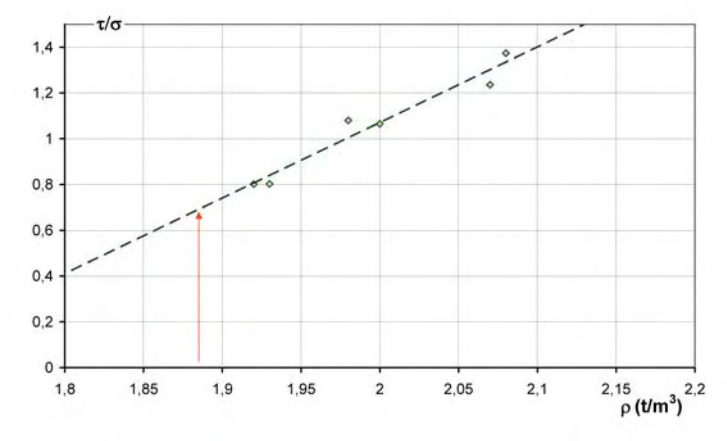

respect to a single parameter, namely the dry mass density or, equivalently, the void index, by writing the relation in the following form:

$$\tau_f/\sigma_n = \tan \varphi_\mu + \lambda_r (\sigma_n) * (\rho_d - \rho_{d\,min}) \quad (3)$$

with:

- $\tan \varphi_\mu = 0.72$

- $\rho_{d\,min} = 1.88$ t/m^3, for $(c'\text{-}c_0) = 0$, according to **Figure 17**.

Figure 18 presents two sets of results from precision triaxial tests using the 150-mm diameter. In general, the values of initial tangent moduli (E_{tan}) obtained for both the embankment material and leveled materials lie below those derived using the recomposition techniques; this difference however diminishes slightly when focusing on the E_{cycl} unloading-reloading modulus values **(see Table 3)**. This difference cannot be fully explained by the compaction objective (98% of NPO for laboratory recompositions and 95% of NPO for the embankments) since the ultimate densities observed lie very close to one another, as will be seen further below.

figure 18
Triaxial test with unsaturated CD precision - σ'_3 = 50, 100 and 150 kPa

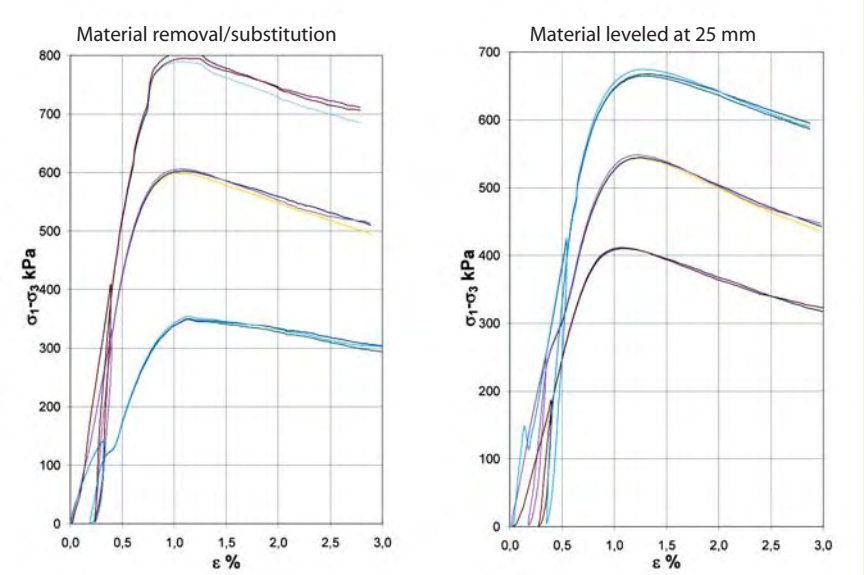

table 3
Results from the triaxial tests σ_3 = 100 kPa (d_{max} = 25 mm)

Material	Compaction	E_{tan} (MPa)	E_{cycl} (MPa)
Embankment - 2nd layer	Roller	33.8	117.3
Embankment - 1st and 2nd layer	Roller	24.7	-
Embankment material	Static	66.5	134.0
Laboratory - leveled	Static	73.1	141.5
Laboratory - removal/substitution	Static	92.8	178.6

Influence of water content on failure

In order to test the influence of water content on shear box test results, the material was compacted at various water contents. The Proctor characteristics of the $0/d_{max}$ = 0/50 mm fraction are a water content w_{OPN} = 7.1% and an optimal density γ_{NPO} = 2.13. The spacing between boxes has been maintained at t = 25 mm.

The results from **Table 4** show, on the CER Center's shear box, a decrease in the peak angle of friction on the order of 6 degrees and a drop in cohesion as well, in the neighborhood of 18 kPa for a

table 4
Shear box test results

Test	Operator	Box (mm)	w (%)	γ_d (kN/m³)	c (kPa)	φ (degrees)
CER-4	Vallé	500	6.3	20.9	65.3	45.6
CER-7	Afriani	500	7.5	19.5	46.0	39.4
LRL-1	Subrin	600	7.1	19.5	57.8	37.5
LRL-2	Subrin	600	6.6	19.5	66.0	38.4
LRL-3	Subrin	600	8.7	20.7	67.5	43.7
LRL-6	Subrin	600	6.4	20.5	89.5	44.9
LRL-7	Subrin	600	7.5	19.5	71.6	38.2
LRL-10	Subrin	600	8.6	19.4	26.7	40.0
LRL-11	Subrin	600	10.9	19.6	14.7	42.2

water content rise from roughly 6.3% to 7.5%. This trend had been previously detected by Shirdam *et al.* **[11]** with a fall of 2.1 degrees and 39 kPa, respectively, with a water content increase from 6.9% to 9.25% for limestone rockfall debris compacted in the shear box with a 600-mm circular cross-section at a relatively similar dry density.

The results obtained by Subrin and Chapeau **[25]** are displayed in **Figure 19**, where cohesion and angle of friction are graphed vs. water content. The angle of friction indicates a contradictory variation, yet of small magnitude, between the two test series with unit weights of 19.5 and 20.5 kN/m³. On the other hand, the drop in cohesion is very distinct, reaching 50 kPa for a 4.5% increase in water content, at constant unit weight (it should be noted that the LRL-7 test from **Table 4** refutes this observation).

Beyond the artifact produced by the instrument itself, the high cohesion values, lying on the order of 50 to 100 kPa at low water content levels, might also be explained at least in part by the non-saturation effect which incites the phenomena of capillarity and suction within samples. The water content increase also leads to transitioning from a qualitatively dilatational behavior of the material during shear (sharp peak with a volume increase) to a contracting type of behavior (peak reached as a residual, volume decrease). These observations are correlated with the material consolidation stress generated by compaction, with this phenomenon identified both *in situ* and in the laboratory.

figure 19
Influence of water content on the shear strength parameters:
- a) cohesion
- b) angle of friction

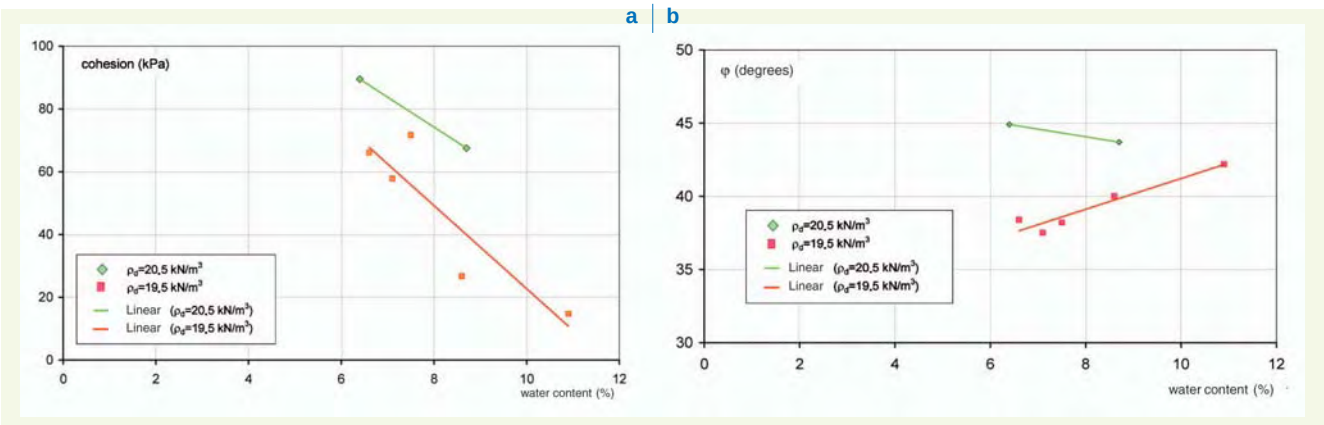

Influence of compaction mode on the density

In order to verify mass density homogeneity over the entire triaxial specimen height, the specimens were submitted to a diagnostic evaluation on the gamma-densitometer bench with measurements conducted at 1-centimeter intervals along a generatrix line. It is straightforward to observe the

interlayer zones with density peaks. The densities are higher for compactions using the "vibrating hammer" and the "Proctor", while they prove to be lower for the vibratory compression; in all cases however, they lie close to the value of NPO, i.e. $\rho_d = 2.03$. The specimen cut into the embankment reveals a sharp density drop at the bottom of the layer, which is quite common (**see Fig. 20**).

To ensure embankment quality following its construction, two of its points were examined using the dual probe down to a depth of 1.0 m. The water content was determined every 10 cm by sampling material using a handheld auger. For any embankment height, the water content varied from 8.4 to 10.0%, with an average of 9.3%, while mass density ranged from 1.86 to 2.03 Mg/m^3 at individual points with an average of 1.96 Mg/m^3 and a compaction rate (CR) of 96.7%.

The three penetrograms derived on the embankment all indicate the same trends and reveal that the compaction obtained is of high quality given that the resultant curves lie to the right of the reference curve q_4 throughout the profile **(Fig. 21)** **[19]**.

figure 20
Mass density profiles for:
a: the embankment
b: the triaxial specimens

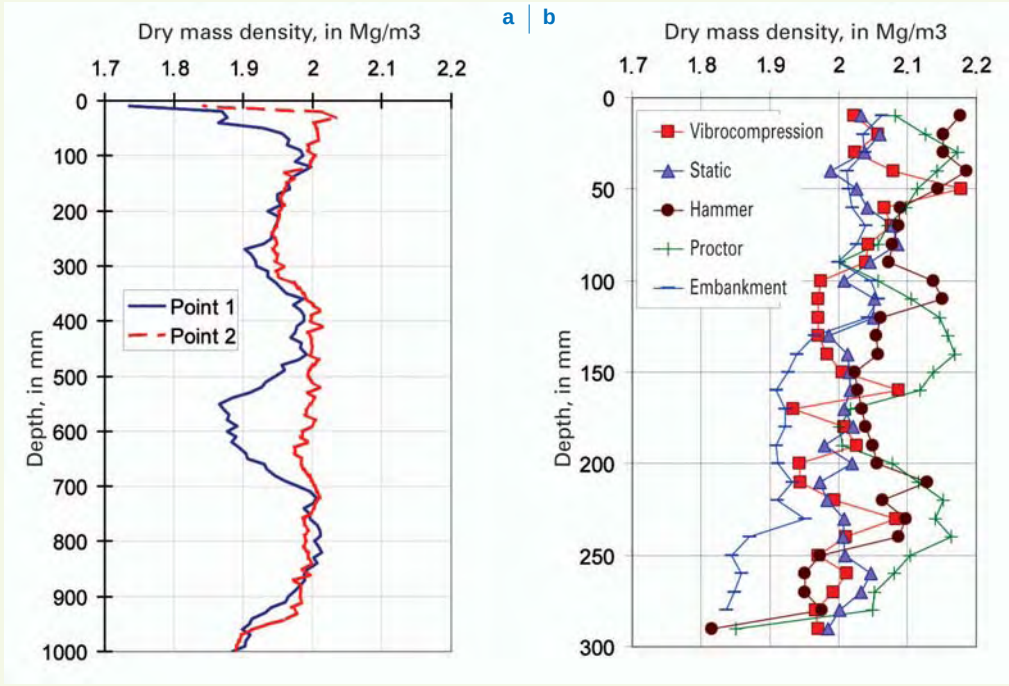

figure 21
Penetrometric profiles and reference curves (according to **[19]***)*

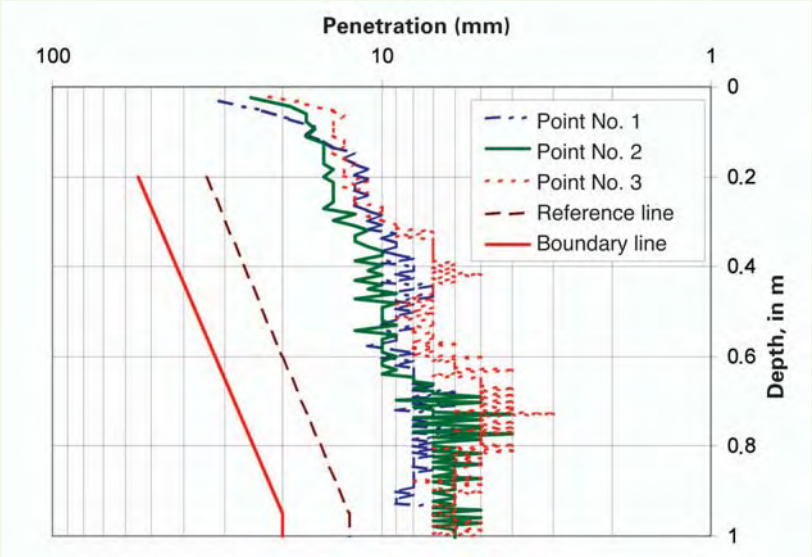

Influence of compaction mode on mechanical parameters

The stress-strain curves from triaxial tests are shown in **Figure 22** for each compaction protocol, on specimens produced in the laboratory and extracted from the embankment.

The intrinsic curves on **Figure 23** depict the evolution in the material's cohesion and angle of internal friction derived from the triaxial test results for various compaction modes.

According to **Table 5** and **Figure 23**, the cohesion and angle of friction values are near constant, except for the Proctor and embankment compaction, for which cohesion is lower and the angle of friction higher. This finding may be explained by the variation in material characteristics for Proctor and embankment compaction in comparison with the other modes. While the materials do in fact stem from the same origin, they differ due to natural site variability **[4]**.

The shear strength of the investigated soil is thus only marginally affected by the process for preparing triaxial test specimens, despite the presence of density and water content gradients all along the specimens. In contrast, the tangent modulus is much more sensitive to the specimen compaction mode, with variations exceeding 100% **(see Fig. 22** and **Table 5)**. This finding demonstrates that the means employed to compact a material exert significant impact on its deformation behavior. Strain

figure 22
Stress-strain curves derived from the triaxial test with 150-mm specimens, Unsaturated CU - σ'_3 = 100 kPa

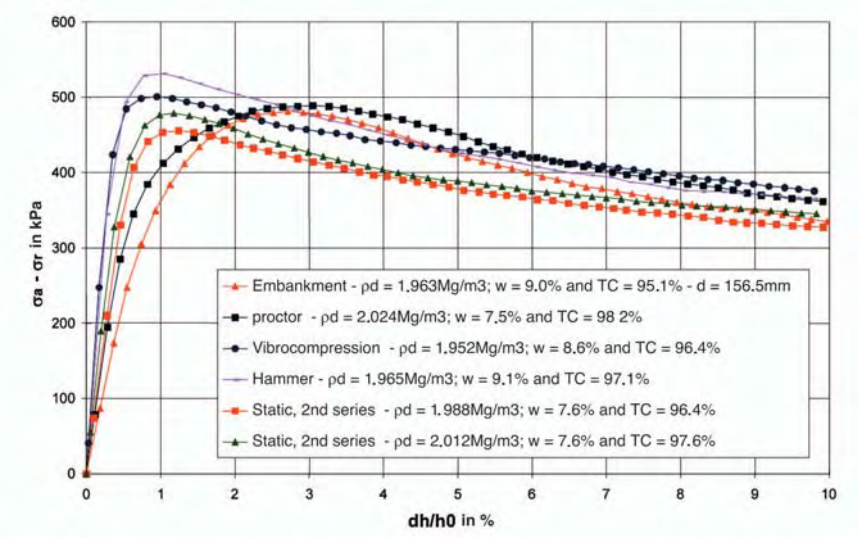

figure 23
Intrinsic curves for the triaxial test

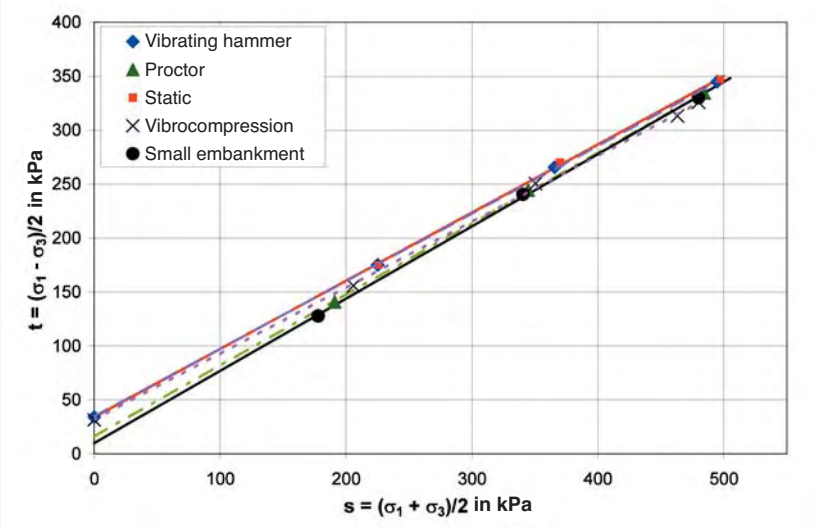

table 5
Results from triaxial tests for σ_3 = 100 kPa (peak strength)

Mode	c (kPa)	φ (degrees)	E_{tan} (MPa)
Hammer	43.8	39.0	125.8
Static	43.8	39.2	64.1
Vibrocompression	39.7	37.8	116.0
Proctor	20.9	41.2	89.3
Embankment	13.4	42.0	43.0

hardening or overconsolidation phenomena likely play a role in these different compaction modes. A series of repetitiveness tests (not presented herein) were conducted and did yield satisfactory results **[4,25-26]**.

Influence of test equipment shape

The tests performed using the square section direct shear box produced by the CER Center were replicated in the circular section direct shear box at the regional Lyon laboratory. These tests are not strictly identical however, given the variations in water content *w* and unit weight γ_d with respect to the CER values; moreover, a wider confinement stress domain was proposed by the Lyon lab.

The initial conditions in test LRL-6 make it comparable to the CER-4 test carried out by Vallé **[4]** (see **Table 4**). **Figure 24** summarizes the criteria from both tests in terms of peak and residual strengths for a given vertical stress domain. At the peak, the shear stresses measured with the 600-mm circular box are systematically higher than those measured with the 500-mm square box, by roughly 10 to 30 kPa, despite a slightly higher dry unit weight for the Vallé test **[4]**. The interpretation at peak strength leads to a deviation in cohesion on the order of 25 kPa and a deviation in angle of friction of less than 1 degree.

In terms of residual strength, results are similar, except for a vertical stress σ_v = 250 kPa, for which a 20-kPa deviation on shear strength is recorded. The impact on mechanical characteristic values is reflected by a deviation of approx. 10 kPa for cohesion and of less than 2 degrees for the angle of friction. While this latter deviation has been evaluated consistently between the two set-ups, cohesion remains a highly variable parameter depending on whether the interpretation is provided in terms of peak or residual strength.

figure 24
Intrinsic curves obtained for various test devices

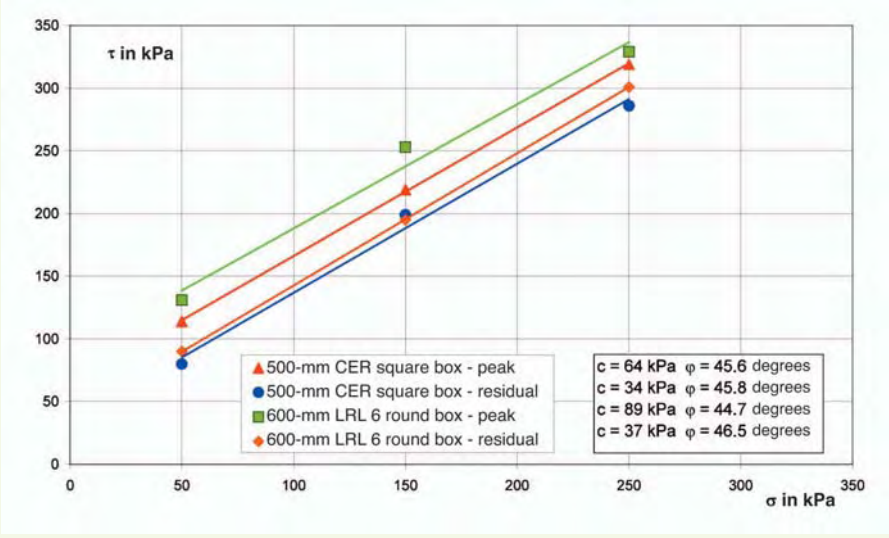

Results from the LRL-6 test are also influenced by the shear box roughness. Installation of a peripheral cladding made of Teflon, which limits friction at the interface between shear box and sample, in reality systematically incites a reduction in shear strength and hence yields similar results with both measurement systems.

Thanks to these comparative tests, the discrepancies related to test repeatability, and in particular on shear stress values, have been highlighted. On the other hand, the overall interpretation of a shear test does lead to rather consistent results. Deviations lying on the order of 10 to 20 kPa for cohesion and 1 to 2 degrees for angle of friction can be observed between the two systems.

Influence of measurement equipment size

Conducting shear box and triaxial tests for various specimen geometries allows drawing a number of conclusions regarding the influence of equipment size on test results for coarse-grained material. The tests performed at the CER Center using two sizes of square section direct shear boxes (see **Table 2** and **Fig. 15)** have provided very similar results. Deviations of a few kPa for cohesion and 1-2 degrees for angle of friction can be observed between the two equipment sizes.

Table 6 lists the references and characteristics of specimens produced in the laboratory for running the triaxial revolution tests on specimens composed of material leveled at 25 mm with diameters of 150 mm and 300 mm. These two test series focus on a material of identical origin, even though natural variations from one sampling site to the next have to be taken into account.

The stress-strain curves, measuring excess pore pressure vs. axial strain, i.e. the σ'_1/σ'_3 ratio as depicted in the Lambe plane **(Fig. 25)**, yields for the test on the 300-mm diameter with Criquebeuf-sur-Seine gravel leveled at 25 mm a cohesion of 9 kPa and an angle of friction equal to 36.5 degrees, i.e. for a 10-kPa drop in cohesion and a 4.6-degree decrease for angle of friction in comparison with the tests performed on the 150-mm specimen.

The 150-mm specimens exhibit a rather distinct failure plane, and the angle of inclination varies from 50 to 56 degrees for all specimens **(Fig. 26a)**. In the case of compaction steps applied in three layers, the failure plane sometimes crosses the interface lying between the first and second layers.

This failure localization is not observed on the 300-mm specimens, all other things held the same, i.e.: particle size distribution, compaction mode, number of layers **(Fig. 26b)**. Consequently, the lack of influence from the largest grains on the separation of particles within the failure surface plane upon reaching the critical state could explain the shape of the stress deviator vs. strain curves, in which no peak is apparent, in addition to the absence of cohesion during analysis in the Mohr-Coulomb plane. Another possible explanation naturally pertains to a lower density obtained on the larger specimens; specimen mass densities nonetheless lie between 1.95 and 2.09 t/m^3, which compares well with mass densities varying from 1.96 to 2.02 t/m^3 for the 150-mm specimens. Furthermore, this conclusion, which ties the evolution in parameters to specimen size, would seem to be corroborated by the drop in cohesion remarked by Vallé **[4]** during shear box tests using decreasing values of the material leveling diameter (see **Table 2)**. This observation cannot be made however when comparing tests with different box sizes, as discussed above, since the spacing (t) is held constant. This evolution in cohesion vs. spacing has been confirmed in several studies **[4,12,25-27]**.

Influence of the type of shear test

Table 6 lists the parameters obtained from all of the tests conducted. A high level of consistency can be noted in these results **(Fig. 27)**.

Differences at the level of deformation or failure parameters are seen to depend on how the measurement equipment has been loaded; moreover, it has been observed that, under current

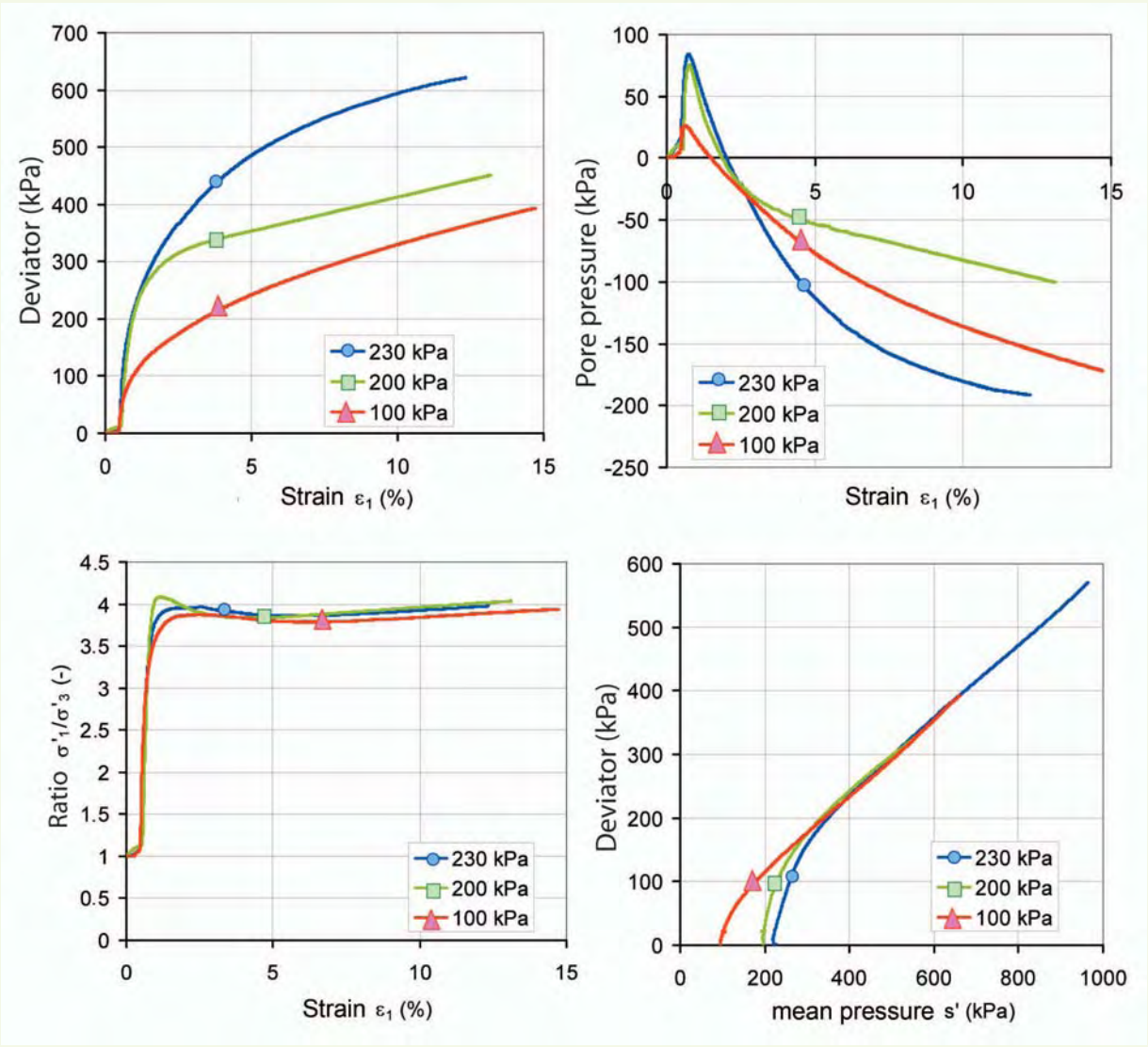

figure 25
Results from the triaxial test using the 300-mm diameter specimen for the Criquebeuf-sur-Seine material leveled at 25 mm

figure 26
Deformed specimens after triaxial tests with the a) 150-mm specimen; and b) 300-mm specimen

implementation conditions, the direct shear box test displays greater dispersion than the triaxial test. It proves more difficult to reproduce since the equipment boundary conditions and procedures applied across the various laboratories vary too widely. In addition, this test tends to overestimate material cohesion as a result of the excessive influence from the effect of interlocking grains on results

table 6
Results for various types of tests on the embankment material (roller compaction except for the box: hammer)

Test	c (kPa)	φ (degrees)	E_{tan} (MPa)	E_{cycl} (MPa)
Box - square 500 mm	57.5	38.9	-	-
Triaxial - 150 mm	43.8	39.0	37	117
Triaxial - 150 mm *	-	-	17.5	42.2
Triaxial - 300 mm	9.0	36.0	95	-
Plate	-	-	19.9	41.9
Pressuremeter	-	-	13.8	37.2

* Modulus values estimated like for the plate modulus

figure 27
Intrinsic curves for various test devices (d_{max} = 25 mm - hammer compaction)

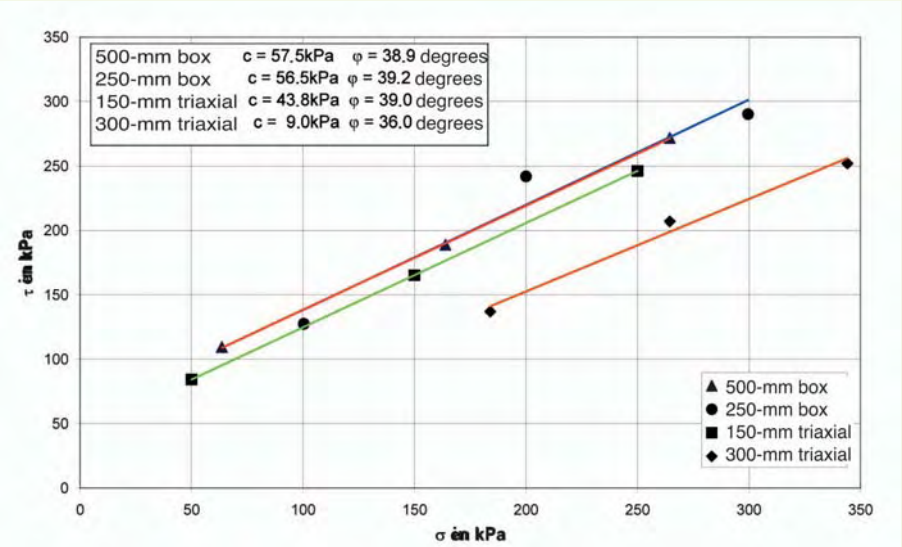

(Table 6). The cohesion recorded with the shear box decreases almost linearly with the increase in spacing. Subrin and Chapeau noted a cohesion of around 50 kPa for t = 25 mm and a value of 10 kPa for t = 50 mm **[23]**. In contrast, the angle of friction is little influenced by spacing t.

CONCLUSION

This series of experimental research campaigns have demonstrated that the type of test device employed does play a role in the material strength observed. The ratio between test equipment dimensions and grain size must have a minimum threshold in order not to influence results. The test results presented herein lead to suggesting that the L_0/d_{max} ratio[1] must exceed 15 or 20 for the direct shear box when the material displays a flat particle size distribution curve and twice this number when the graduation is more uniform. For the triaxial device, the D_0/d_{max} ratio[1] must at least equal 6 and even higher as the material shows a more uniform particle size graduation.

For tests performed with the direct shear box, an increase in soil strength parameter values has been observed; angle of friction and cohesion values rise as the maximum grain diameter d_{max} increases; this growth in d_{max} is accompanied by an increase in uniformity coefficient (C_U). The leveled and recomposed materials have yielded relatively similar values for both cohesion and angle of internal friction; the values obtained range between 56 and 65 kPa for cohesion and between 39 and 45 degrees for angle of friction (when using Lo = 500 mm). The materials were tested using the same mass densities. The direct shear box test leads to very high values for cohesion, which in this instance is referred to as “apparent cohesion”. Comparative testing conducted with a large round box and a large square box have exposed deviations on the order of 10 to 20 kPa for cohesion and

[1] *L_0 is the maximum dimension of the shear box and D_0 is the maximum specimen diameter.*

1-2 degrees for angle of friction. The cohesion deviation more than doubles when varying the spacing from $d_{max}/2$ to d_{max}. Whether examining the measurement cell shape or size, the influence of the measurement equipment does not seem to be as strong as the spacing between the two half-boxes. It can thus be concluded that the recommended spacing of $d_{max}/2$ is not sufficient to eliminate cohesion due to grain interlocking. The required spacing would be in the vicinity of d_{max}.

The peak soil shear strength, as measured from the triaxial tests, is relatively unaffected by the specimen production process; the values obtained range between 13 and 44 kPa for cohesion and 38-42 degrees for angle of friction. The tangent modulus is much more sensitive to specimen compaction mode, with the values yielded extending from 30 to 130 MPa, depending on specimen origin (i.e. produced in the laboratory or cut onsite from the embankments). The angle of internal friction values for the leveled materials are much smaller than those observed for the material recomposed by removal and substitution, while cohesion values are nearly the same. The material recomposed by means of removal and substitution was tested for higher mass densities than those of the leveled materials due to how the various particle fractions are arranged differently **[28]**.

The dimensional distribution of grains, i.e. the test particle size distribution, constitutes another parameter to be taken into account when testing coarse-grained soils in the laboratory. Leveling is the simplest process, yet a recomposition method consisting of removing the coarsest part of the material and substituting with a material sized between 5 mm and d_{max} has been employed. From results produced by both the box and triaxial tests, it is observed that for leveling and recomposition by removal and substitution, strength parameter values differ if the mass density also differs; otherwise, the values obtained are indeed similar. The process adopted to derive a given particle size distribution can however lead to arranging and overlapping grains differently in the soil mass, which in turn could generate different types of soil behavior.

On the whole, this experimental study revealed that the cohesion values obtained based on direct shear box tests are higher than those stemming from the triaxial tests. For the angle of friction, the values are close to one another.

It would thus seem necessary, subsequent to this study, to propose developing standards that limit the reliance upon leveling or substitution of the coarsest particle size fraction in mechanical characterization tests. This step could be performed within the scope of work underway by Technical Committee 341 of the European Standardization Committee assigned to establish an NPO density test standard specific to soil mechanics testing.

This research has made it possible to highlight the risk of overestimating cohesion when applying a compaction mode that leads to excessive density or during shear box tests with an inappropriate geometry. It thus proves necessary to adapt the experimental practice to coarse-grained soils in order to preserve an adequate safety dimension for slopes and geotechnical structures.

ACKNOWLEDGMENTS

The authors would like to thank their colleagues Nilton Vallé, Jean-Claude Blivet, Lusmeila Afriani, Dominique Lozach and Assia Ghemmour with the CETE Normandy-Centre Research Center, as well as Simon Pouget from the regional Ponts et Chaussées laboratory in Lyon, who all contributed to this project through participating in research steps or providing valuable advice.

REFERENCES

1 **Perrot A.**, *Étude de la résistance au cisaillement des sols grossiers*, étude bibliographique 68.B.113, **1968**, LCPC, 50 pages.

2 **Ursat P.**, **Saint R.**, *Étude de la résistance au cisaillement d'une grave argileuse*, rapport du Laboratoire régional de Rouen, **1970**, 30 pages.

3 **Camapum de Carvalho J.**, **Mieussens C.**, **Queiroz de Carvalho J.-B.,** Problèmes de reconstitution des éprouvettes de sol en laboratoire - Proposition d'une méthode, *Bulletin de liaison des laboratoires des ponts et chaussées*, **1985**, **135**, pp. 77-83.

4 **Vallé N.**, *Comportement mécanique d'un sol grossier d'une terrasse alluvionnaire de la Seine*, Thèse de doctorat, université de Caen/Basse Normandie, **2001**, 287 pages.

5 **Fry J.-J.**, **Flavigny E.**, Classification et propriétés des enrochements : le cas d'un grès, *Proceedings of the twelfth international conference on soil mechanics and foundation engineering*, Rio de Janeiro, **1989**, vol. **1**, pp. 713-714.

6 **Santos**, **Martinez**, **Garcia**, Efecto en los esayos de laboratorio de propriedades resistentes de materiales granularees, *Simposio sobre geotecnia de presas de materiales sueltos*, Zaragoza, **1993**, pp. 117-122.

7 **Fumagalli E.**, Tests on cohesionless materials for rockfill dams, *Journal of the soil mechanics and foundations division*, Trans. american society of civil engineers (ASCE), **1969**, vol. **95**, nº SM1, pp. 313-330.

8 **Holtz W.-G.**, **Gibbs J.**, Triaxial mechanics tests on previous gravelly soils, *Journal of the soil mechanics and foundation division*, ASCE, **1956**, vol. **82**, paper **867**, pp. 1-22.

9 **Laréal P.**, **Bourdeau Y.**, **Lambert P.**, **Cottereau Cl.**, Essais de cisaillement *in situ* sur des sols alluvionnaires de la vallée du Rhône, *Travaux*, **1973**, n° **459-460**, pp. 52-59.

10 **Bourdeau Y.**, **Laréal P.**, **Marchal J.**, Résistance au cisaillement des alluvions du Rhône, *Proceedings of the twelfth international conference on soil mechanics and foundation engineering*, Rio de Janeiro, **1989**, vol. **1**, pp. 695-696.

11 **Shirdam R.**, **Faure R.-M.**, **Magnan J.-P.,** *Comportement mécanique des matériaux superficiels des versants naturels*, **2001**, ERLPC, GT71, 210 pages.

12 **Shirdam R.**, *Comportement mécanique des matériaux superficiels des versants naturels*, Thèse de doctorat, Institut national des sciences appliquées de Lyon, **1998**.

13 **Afnor**, norme **NF P 94-074**, *Essai à l'appareil triaxial de révolution - Appareillage, préparation des éprouvettes,* essais UU, CU + u, CD, **1994**.

14 **Charles H.**, Triaxial géant, *Bulletin de liaison des laboratoires des ponts et chaussées,* **1968**, **35**, pp 20-22.

15 **Vallé N.**, **Blivet J.-C.**, **Khay M.**, **Reiffsteck Ph.**, Méthode de compactage appliquées aux matériaux alluvionnaires, *6e journées nationales Génie civil - Génie côtier*, Caen, **2000**, tome **2**, pp. 337-348.

16 **Reiffsteck Ph.**, **Blivet J.-C.**, **Vallé N.**, **Khay M.**, Écueils de la mesure en laboratoire du comportement mécanique des sols grossiers, *15th international conference on soil mechanics and foundation engineering*, Istanbul, Balkema, **2001**, pp. 255-259.

17 **Bertaina G.**, **Blivet J.-C.**, **Reiffsteck Ph.**, **Chapeau C.**, **Hervé S.**, **Canou J.**, **Khay M.**, **Mestat Ph.**, **Garcia P.**, *Opération 1J991 Comportement des matériaux grossiers*, Rapport final d'opération, **2004**, 120 pages.

18 **Dupla J.-C.**, **Pedro L.-S.**, **Canou J.**, **Dormieux L.**, Comportement mécanique des sols grossiers de référence, *Bulletin des laboratoires des ponts et chaussées*, **2007**, **268-269**, pp.

19 **Sétra-LCPC**, *Guide des terrassements routiers. Réalisation des remblais et des couches de forme,* **1992**, 90 pages.

20 **Hintzy,** *Triaxial grand modèle, expérimentation*, **1969**, PV n° **4310**, 57 pages.

21 **Ghemmour A.**, *Sols hétérogènes : caractérisation et comportement mécanique*, diplôme de Master 2 recherche option Génie côtier, université de Caen/Basse Normandie, **2005**, 91 pages.

22 **Arbaut J.**, *Caractérisation mécanique des matériaux hétérogènes*, mémoire d'ingénieur CNAM, **2007**, 50 pages (à paraître).

23 **Jamiolkowski M.-B.**, **Lo Presti D.C.F.**, Shear strenght of coarse soils from in situ tests a compendium, *the fourth international geotechnical engineering conference*, Cairo, **2000**, pp. 1-41.

24 **Monnet J.**, **Khlif J.**, Étude théorique et expérimentale de l'équilibre élasto-plastique d'un sol pulvérulent autour du pressiomètre, *Revue française de géotechnique*, **1994**, n° **67**, pp. 3-12.

25 **Subrin D.**, **Chapeau C.**, *Essais à la grande boîte de cisaillement pour sols grossiers, Essais croisés sur la grave alluvionnaire de Criquebeuf-sur-Seine,* rapport LCPC, **2006**, 102 pages.

26 **Afriani L.**, *Essais de cisaillement direct des sols grossiers : incidences des procédures d'essai et effets d'échelle,* Thèse de doctorat, université de Caen, **2003**.

27 **Levacher D.**, **Khay M.**, **Lozach D.**, **Afriani L.**, Caractérisation de la résistance au cisaillement d'un sol grossier – Application à une grave alluvionnaire, In Shahrour I., Kazan Y., Gambin M., Lancelot L. Eds, Proceedings of *the international conference on geotechnical engineering*, Beyrouth, **2004**, pp. 703-709.

28 **Reiffsteck Ph.**, **Nguyen Pham P.-T.**, **Arbaut J.**, Influence de la répartition granulométrique sur le comportement mécanique d'un sol, *Bulletin des laboratoires des ponts et chaussées*, **2007**, **268-269**, pp.